Original Research

Visualization of Hemodynamics in Intracranial Arteries Using Time-Resolved Three-Dimensional Phase-Contrast MRI

Shuhei Yamashita, MD,[1]* Haruo Isoda, MD, PhD,[1] Masaya Hirano, MS,[2] Hiroyasu Takeda, RT,[1] Shoichi Inagawa, MD,[1] Yasuo Takehara, MD, PhD,[1] Marcus T. Alley, PhD,[3] Michael Markl, PhD,[4] Norbert J. Pelc, ScD,[3] and Harumi Sakahara, MD, PhD[1]

Purpose: To visualize the hemodynamics of the intracranial arteries using time-resolved three-dimensional phase-contrast (PC)-MRI (4D-Flow).

Materials and Methods: MR examinations were performed with a 1.5T MR unit on six healthy volunteers (22–50 years old, average = 30 years). 4D-Flow was based on a radiofrequency (RF)-spoiled gradient-echo sequence, and velocity encoding (VENC) was performed along all three spatial directions. Measurements were retrospectively gated to the electrocardiogram (ECG), and cine series of three-dimensional (3D) data sets were generated. The voxel size was $1 \times 1 \times 1$ mm, and acquisition time was 30–40 minutes. 4D data sets were calculated into time-resolved images of 3D streamlines, 3D particle traces, and 2D velocity vector fields by means of flow visualization software.

Results: We were able to see the 3D streamlines from the circle of Willis to the bilateral M2 segment of the middle cerebral arteries (MCAs). Time-resolved images of 3D particle traces also clearly demonstrated intracranial arterial flow dynamics. 2D velocity vector fields on the planes traversing the carotid siphon or the basilar tip were clearly visualized. These results were obtained in all six volunteers.

Conclusion: 4D-Flow helped to elucidate the in vivo 3D hemodynamics of human intracranial arteries. This method may be a useful noninvasive means of analyzing the hemodynamics of intracranial arteries in vivo.

Key Words: intracranial arteries; hemodynamics; flow visualization; MR imaging; phase-contrast MR imaging
J. Magn. Reson. Imaging 2007;25:473–478.

THERE ARE MANY FACTORS other than genetics that affect the occurrence and progression of vascular disease. Hemodynamics is suspected to be one of the main factors, since vascular diseases such as atherosclerosis and intracranial aneurysms usually develop near the vascular bifurcation (1–3). The results of many in vitro hemodynamic experimental methods, including dye injection (4–6), laser Doppler velocimetry (LDV) (7–9), phase-contrast (PC)-MRI (10), tagged MRI (11), and tagged MRI analyzed by particle image velocimetry (PIV) software (12), depend on experimental conditions, such as the flow rate of the fluid and proper replication of the vascular wall motion. Because of these limitations, it is very difficult to reproduce in vivo blood flow in in vitro experiments with guaranteed accuracy. In addition, it is difficult to measure in vitro hemodynamics for each model created according to each patient's vascular structure. In recent years, computer simulations have been used frequently to visualize the hemodynamics of intracranial arteries (13–17). It is debatable, however, whether a computer simulation can accurately reflect in vivo hemodynamics, since the results depend on certain assumptions and the setting of boundary conditions. Because of these limitations, a method for direct measurement of in vivo hemodynamics is desirable.

Two methods for in vivo analysis of intracranial hemodynamics are transcranial Doppler (TCD) (18) and two-dimensional (2D) cine PC-MRI (19). Both of these methods have drawbacks, however. The observable range of TCD is limited and the spatial resolution is

[1]Department of Radiology, Hamamatsu University School of Medicine, Shizuoka, Japan.
[2]GE Yokogawa Medical Systems, Tokyo, Japan.
[3]Department of Radiology, Stanford University School of Medicine, Stanford, California, USA.
[4]Department of Diagnostic Radiology, Medical Physics, University Hospital Freiburg, Freiburg, Germany.
Presented at the 13th Annual Meeting of ISMRM, Miami Beach, FL, USA, 2005.
*Address reprint requests to: S.Y., Department of Radiology, Hamamatsu University School of Medicine, 1-20-1 Handayama, Hamamatsu, Shizuoka 431-3192 Japan.
E-mail address: shuheiy@hama-med.ac.jp
Received October 5, 2005; Accepted September 27, 2006.
DOI 10.1002/jmri.20828
Published online 5 February 2007 in Wiley InterScience (www.interscience.wiley.com).

insufficient. The results of TCD also depend to a large degree on the technique used and the skill of the examiners. 2D cine PC-MRI has been used for a long time, but the blood-flow analysis was done for a limited number of slices. Acquiring three-dimensional (3D) velocity profiles of intracranial arteries within a clinically applicable time would be useful for the management of patients with intracranial arterial diseases.

The time-resolved three-dimensional PC-MRI (4D-Flow) method, which can acquire four-dimensional (three spatial dimensions and one time dimension) hemodynamic data, and depict aortic hemodynamics (e.g., velocity vectors and 3D streamlines) was recently developed (20,21). In the present study we sought to determine whether we could calculate in vivo intracranial velocity vector fields and visualize in vivo intracranial hemodynamics.

MATERIALS AND METHODS

MR examinations were performed on six healthy volunteers (five males and one female, 22–50 years old, average = 30 years). All studies were approved by our institutional review board, and informed consent was obtained from each volunteer.

The examinations were performed with a 1.5T MR unit (Signa Infinity Twinspeed with Excite XI, version 11; General Electric Medical Systems, Milwaukee, WI, USA) utilizing 4D-Flow. The technique was based on a radiofrequency (RF)-spoiled gradient-echo sequence, and velocity encoding (VENC) was performed along all three spatial directions. Segmented acquisition was used, and measurements were gated for each volunteer's electrocardiogram (ECG) retrospectively. We obtained 20 time frames of 3D data for magnitude and VENC in the x, y, and z directions in one ECG cycle. Velocity-encoded data for each direction underwent two corrections. The first correction was for Maxwell phase effects (22). The second was the Markl-Bammer correction (23), which was used to remove the effect of the gradient nonlinearity on the calculated velocity measurements. In this way we were able to acquire 4D data, including the velocity data of the x, y, and z directions and time. (A full explanation of this technique is beyond the scope of this paper. For a detailed explanation, see Ref. 20.) The imaging parameters were as follows: repetition time (TR)/echo time (TE)/number of excitations (NEX) = 5.4 msec/2.3 msec/1, flip angle (FA) = 15°, receiver bandwidth = 62.5 kHz, field of view (FOV) = 16 cm, matrix = 160 × 160, slice thickness = 1 mm, voxel size = 1 × 1 × 1 mm, number of slices = 40, VENC = 60 cm/second, acquisition time = 30–40 minutes, slew rate = 120 mT/m/msec.

The data obtained by 4D-Flow were converted into the data format suitable for the flow visualization software (EnSight; Computational Engineering International, Apex, NC, USA) by personal computer (Intel Pentium4 CPU, 3.2 GHz, 2048 MB RAM, Linux OS) in about 90 minutes. We forwarded the converted data to another personal computer (Intel Pentium4 CPU, 3.2 GHz, 2048 MB RAM, Microsoft Windows XP), and analysis was performed with EnSight. Time-resolved images of 3D streamlines and 3D particle traces from arbitrary planes were generated, and 2D velocity vector fields on arbitrary planes were calculated.

Details of the visualization tools used were described previously (21). Each voxel obtained by 4D-Flow has 3D vector information of velocity. These voxels make up a time-varying velocity vector field. Vector fields are used to model the speed and direction of a moving fluid throughout space. "3D streamlines" are lines that represent flow direction at one point in time on the vector field. A "3D particle trace" is the path a massless particle would follow if it were placed in a time-varying velocity vector field. "3D pathlines" are defined as the integration of the particle traces. "2D velocity vector fields" are arbitrary 2D planes extracted from the 3D imaging volume in which 3D velocities are displayed over time. Each type of depiction is color-coded according to the velocity magnitude and visualized as cine images with 20 time frames during one cardiac cycle.

After the arbitrary plane was selected, the required time for visualization was about two to three minutes. The total visualization time using EnSight was about one hour.

RESULTS

We were able to generate 3D streamlines from arbitrary planes that were perpendicular to the longitudinal axis of intracranial arteries. When we generated 3D streamlines from the C5 segment of the internal carotid artery (ICA), the carotid siphon was clearly visualized (Fig. 1). When we generated 3D streamlines from the C2 segment of the bilateral ICAs and basilar artery, we were able to visualize the circle of Willis, the M2 segment of the bilateral middle cerebral arteries (MCAs), the A2 segment of the bilateral anterior cerebral arteries, and the P3 segment of the bilateral posterior cerebral arteries (Fig. 2).

3D particle tracing was performed from an arbitrary plane, and clear visualization of intracranial arterial hemodynamics was obtained. When we traced flow dynamics from the C5 segment of the ICA, the particles in the carotid siphon were clearly visualized (Fig. 3). The parabolic velocity profile was observed immediately after the generation of particles (Fig. 3a). 3D pathlines showed that the blood flowed in the greater curvature in the curved segment of the arteries (Fig. 3b and c).

We also obtained time-resolved velocity vector maps on arbitrary planes in the intracranial arteries. Velocity vector maps in the region where intracranial aneurysms occur frequently, such as the basilar tip (Fig. 4) and the bifurcation of the internal carotid and posterior communicating arteries (IC-PC) (Fig. 5), were obtained. These results were obtained for all volunteers.

The fastest blood flow was observed in the C1-2 segment of the ICA. The mean maximal flow velocity of this segment was 71.7 cm/second. In the medial surface of the origin of the posterior cerebral artery (PCA), relatively fast blood flow was observed in some volunteers. Blood flow velocity of more than 60 cm/second was observed in six of 12 PCAs in six volunteers.

DISCUSSION

In this study we obtained data regarding intracranial arterial blood flow, including the main intracranial arteries, using an FOV of 160 × 160 × 40 mm, a voxel size of 1 × 1 × 1 mm, and 20 time frames during one cardiac cycle in 30–40 minutes. We obtained 3D velocity vectors on arbitrary planes of human intracranial arteries with cine images using the visualization software EnSight. We were able to visualize human intracranial arterial hemodynamics from any direction as 3D streamlines and 3D particle traces. The 3D streamlines clearly showed that the intracranial arterial flow was laminar, and the 3D particle traces showed that the velocity profile was parabolic. The pathlines showed that the blood flowed in the greater curvature in the curved segment of arteries. Similar hemodynamics were shown in a replica study performed by Kerber and Liepsch (24). However, in the present study we were able to directly obtain in vivo hemodynamic information from living human beings. To our knowledge, this is the first paper to report that in vivo direct analysis of blood flow in living human intracranial arteries clearly demonstrated hemodynamics similar to those of experimental fluid dynamics (EFD) or computational fluid dynamics (CFD).

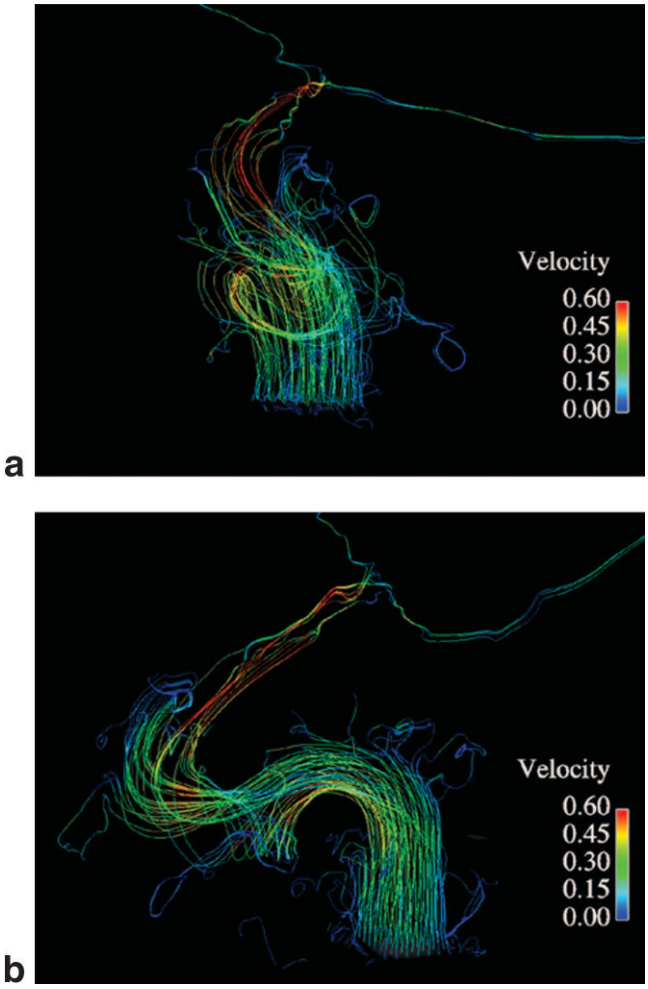

Figure 1. 3D streamlines of the left carotid siphon of a 22-year-old normal male volunteer. An anterior view (**a**) and a left lateral view (**b**) of 3D streamlines on the peak systolic phase clearly demonstrate hemodynamics in the carotid siphon. Streamlines are generated from the C5 segment of the left carotid artery. Images of 3D streamlines can be observed as cine images like a movie on the computer display. Velocities are expressed as a color scale. The unit of the legend is m/second.

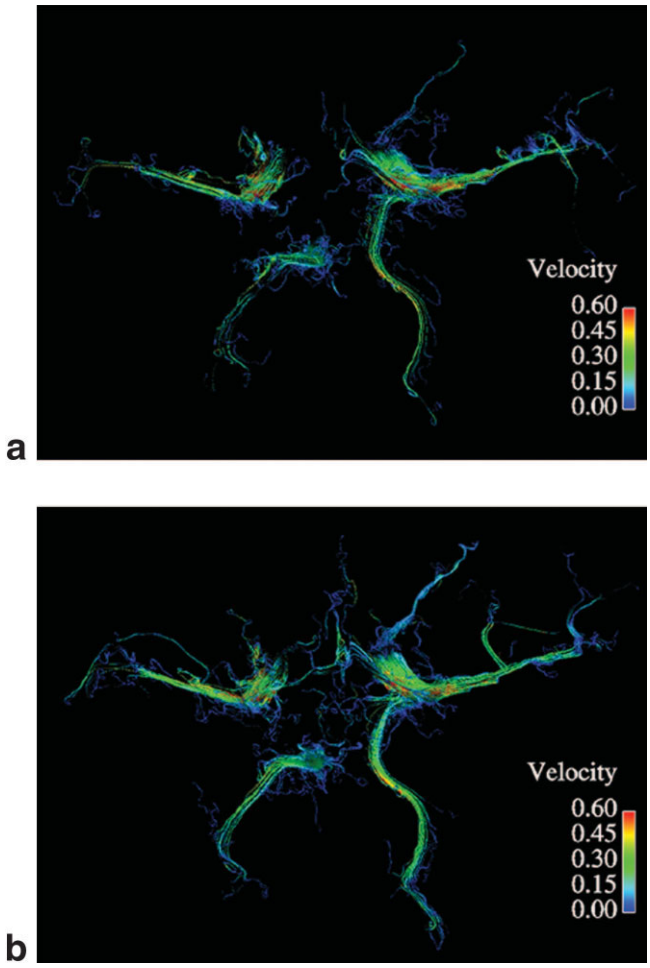

Figure 2. 3D streamlines around the circle of Willis in a 23-year-old normal male volunteer. A craniocaudal view of 3D streamlines around the circle of Willis immediately after the trigger of the R-wave of the ECG (end-diastole, **a**) and 583 msec after the R-wave of the ECG (end-systole, **b**) clearly demonstrate the circle of Willis, bilateral M2 segment of the MCA, bilateral A2 segment of the anterior cerebral artery, and bilateral P3 segment of the PCA. These images can be displayed as cine images like a movie on the computer display. Streamlines were generated from the bilateral ICAs and the basilar artery. Velocities are expressed as a color scale. The unit of the legend is m/second.

The greatest advantage of 4D-Flow imaging is that with this method one can directly and noninvasively measure human intracranial arterial hemodynamics in individual subjects. In EFD and CFD, the results of the hemodynamic analyses of human vessels depend on many variables, such as the shape of the model, periodical movements of the vascular wall, physiological properties of the flowing fluid, and input information of the blood flow profile, including space and time. There-

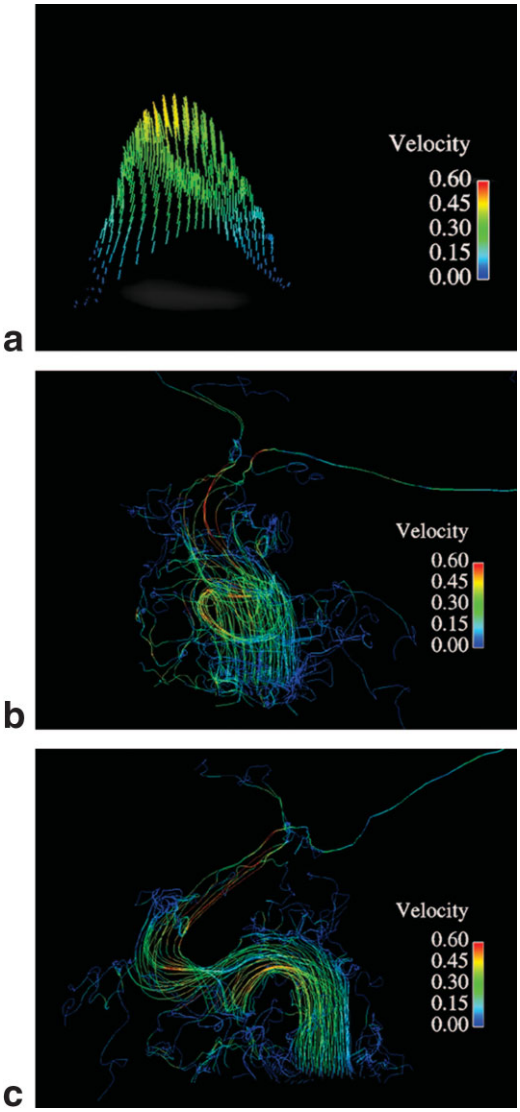

Figure 3. 3D particle traces and 3D pathlines of the left carotid siphon of a 22-year-old normal male volunteer. **a:** A left lateral view of 3D particle traces generated immediately after the trigger of the R-wave of the ECG shows the parabolic velocity profile in the ICA. This finding indicates that the ICA has laminar flow. An anterior view (**b**) and a left lateral view (**c**) of pathlines in which traced particles are connected show that the pathlines are parallel in the straight portion of the vessel, and helical in the region of vessel curvature. Particles are generated from the C5 segment of the left ICA. The colors of the particles and lines represent velocity. The unit of the legend is m/second.

quired for routine MRI. However, it can be done more quickly and less expensively than EFD or CFD. We think that this technique can be applied for in vivo hemodynamic analysis of human intracranial arteries.

However, 4D-Flow has limitations in terms of the imaging time, spatial resolution, temporal resolution, and VENC setting. The acquisition time was dependent on the FOV, matrix, and heart rate (20), and was about 30–40 minutes. Image degradation due to motion may occur during this acquisition time. In the future, it may

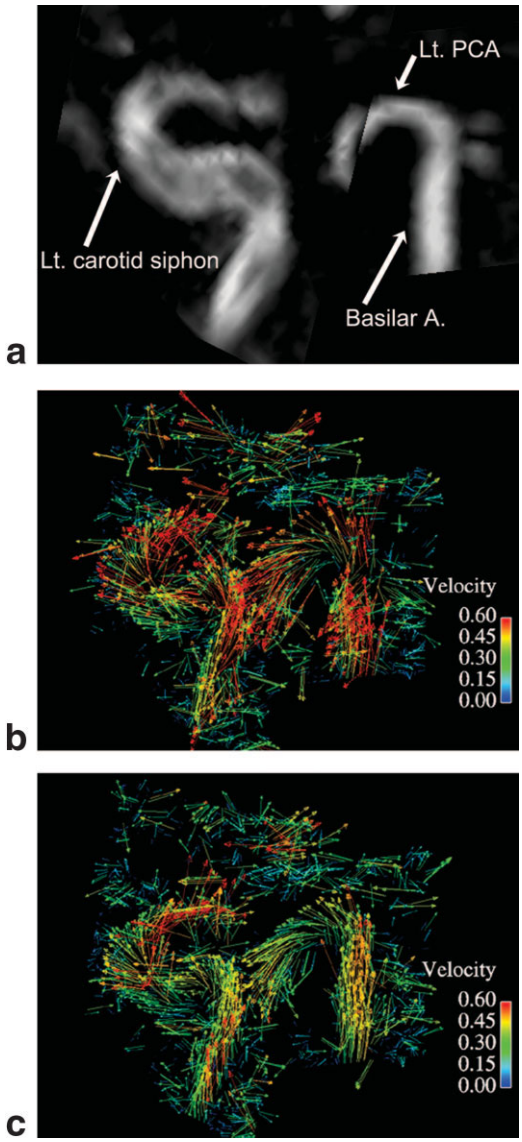

Figure 4. Left posterior oblique views of 2D velocity vector fields on the planes traversing a left carotid siphon and a basilar tip in a 48-year-old normal male volunteer. **a:** Magnitude images traversing a left carotid siphon and a basilar tip show the vascular structure. 2D velocity vector fields immediately after the trigger of the R-wave of the ECG (end-diastole, **b**) and 383 msec after the R wave of ECG (peak-systole, **c**) on the same plane shown in image a clearly show flow vectors around the left carotid siphon and the basilar tip. Flow vectors adjacent to the vascular wall are clearly depicted. The vectors are color-coded according to the velocity shown in the legend. The unit of the legend is m/second.

fore, it is debatable whether these methods can reproduce the actual physiological hemodynamic conditions in living human vessels.

Another advantage of the 4D-Flow method is the shorter time required for imaging and postprocessing, and lower cost compared to EFD and CFD. The imaging time for 4D-Flow in this study was 30–40 minutes, data reconstruction for the visualization software format took 90 minutes, and hemodynamic analysis with the visualization software took about one hour. The acquisition time for 4D-Flow was longer than that re-

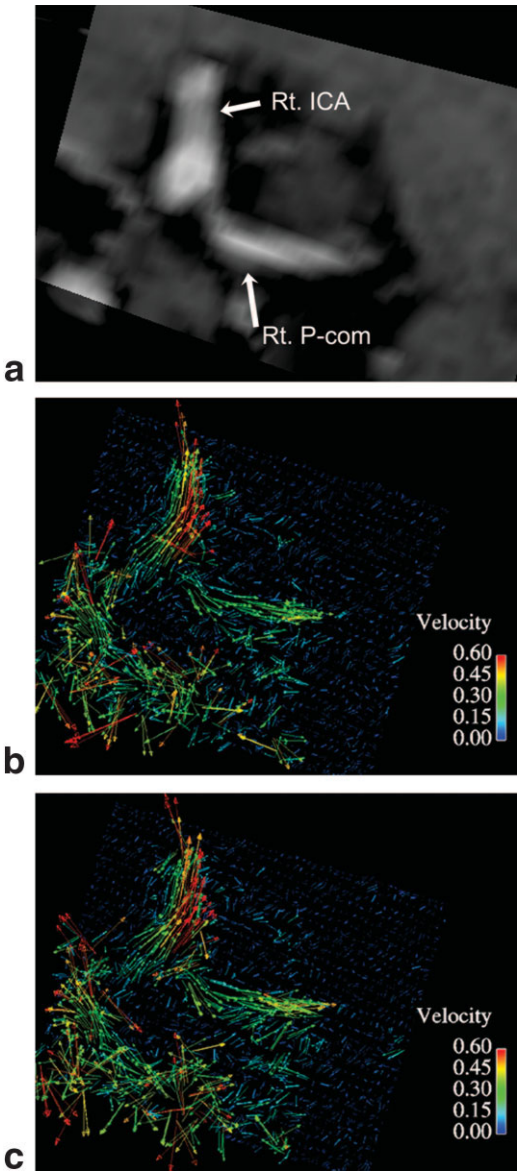

Figure 5. A left lateral view of the 2D velocity vector field on a plane traversing the left IC-PC portion in a 23-year-old normal male volunteer. **a:** A magnitude image traversing the left IC-PC portion shows the shape of the vascular structure. 2D velocity vector fields immediately after the trigger of the R-wave of the ECG (end-diastole, **b**) and 365 msec after the R-wave of the ECG (peak systole, **c**) on the same plane shown in image a clearly show flow vectors around the IC-PC portion. Flow vectors just adjacent to the vascular wall are clearly depicted. The vectors are color-coded according to the velocity shown in the legend. The unit of the legend is m/second.

be possible to shorten the acquisition time by using parallel imaging techniques, coils with a better signal-to-noise ratio (SNR), and improved pulse sequences.

In this study the spatial resolution was $1 \times 1 \times 1$ mm. However, to calculate the wall shear stress properly, we need a voxel size of less than $0.5 \times 0.5 \times 0.5$ mm. High spatial resolution can be achieved using high field magnets and a coil with a high SNR.

In this study, 20 time frames of images were acquired per one heartbeat. Temporal resolution was dependent on the heart rate and was about 40–60 msec. We think this is sufficient for clinical applications. However, the acquisition times for the magnitude image and the x, y, and z components of velocity were slightly different. Also, the acquisition times for adjacent slices were slightly different. To better understand the influence of these differences, fundamental experiments and comparisons between this technique and EFD or CFD will be required. However, in a previous study, Markl et al (20) reported a correspondence between 4D-Flow and 2D cine PC-MRI.

In this study we could only set a uniform VENC, and were unable to change the VENC setting once the examination started. Imaging of slow blood flow is poor at high VENC settings. Reducing the VENC produces good slow-flow images, but the fast flow will be wrapped. In this study we set the VENC to 60 cm/second to observe the slow flow near the vessel wall. Although it is not obvious on our images, there may have been some wrapped data. It is necessary to set VENC appropriately for the area that is being observed.

Although this study included only healthy volunteers, the 4D-Flow technique should be able to analyze the hemodynamics of patients with vascular disease. Wall shear stress is thought to be an important factor in the occurrence and progression of vascular disease. Vascular wall shear stress is defined as the multiplication of fluid viscosity and shear velocity of the neighboring vascular wall. If we can analyze and understand hemodynamics properly and calculate the wall shear stress of normal intracranial arteries, we should be able to predict the occurrence of vascular disease. This 4D-Flow method will play an important role in the measurement of wall shear stress. It may also serve as an important tool for elucidating the mechanisms of occurrence and progression of vascular disease. 4D-Flow data also contain information about the flow volume of the main intracranial arteries. We will be able to use the hemodynamic information of the main intracranial arteries obtained by 4D-Flow as the boundary condition to improve the accuracy of CFD results.

In conclusion, 4D-Flow may be a useful noninvasive method for analyzing the in vivo hemodynamics of the intracranial arteries. With 4D-Flow we were able to gain a better understanding of in vivo 3D hemodynamics in the human intracranial arteries. We obtained data on the in vivo intracranial hemodynamics of living humans in 30–40 minutes. 4D-Flow provided us with time-resolved images of 3D streamlines and 3D particle traces viewed from arbitrary directions, and time-resolved images of 2D velocity vector fields of arbitrary planes.

REFERENCES

1. Malek AM, Alper SL, Izumo S. Hemodynamic shear stress and its role in atherosclerosis. JAMA 1999:282:2035–2042.
2. Rhoton Jr AL. Aneurysms. Neurosurgery 2002:51(4 Suppl):S121–S158.
3. Ingebrigtsen T, Morgan MK, Faulder K, Ingebrigtsen L, Sparr T, Schirmer H. Bifurcation geometry and the presence of cerebral artery aneurysms. J Neurosurg 2004:101:108–113.
4. Kerber CW, Heilman CB, Zanetti PH. Transparent elastic arterial models. I: A brief technical note. Biorheology 1989:26:1041–1049.

5. Kerber CW, Heilman CB. Flow dynamics in the human carotid artery: I. Preliminary observations using a transparent elastic model. AJNR Am J Neuroradiol 1992:13:173–180.
6. Kerber CW, Hecht ST, Knox K, Buxton RB, Meltzer HS. Flow dynamics in a fatal aneurysm of the basilar artery. AJNR Am J Neuroradiol 1996:17:1417–1421.
7. Steiger HJ, Liepsch DW, Poll A, Reulen HJ. Hemodynamic stress in terminal saccular aneurysms: a laser-Doppler study. Heart Vessels 1988:4:162–169.
8. Tateshima S, Murayama Y, Villablanca JP, et al. Intraaneurysmal flow dynamics study featuring an acrylic aneurysm model manufactured using a computerized tomography angiogram as a mold. J Neurosurg 2001:95:1020–1027.
9. Tateshima S, Murayama Y, Villablanca JP, et al. In vitro measurement of fluid-induced wall shear stress in unruptured cerebral aneurysms harboring blebs. Stroke 2003:34:187–192.
10. Tateshima S, Grinstead J, Sinha S, et al. Intraaneurysmal flow visualization by using phase-contrast magnetic resonance imaging: feasibility study based on a geometrically realistic in vitro aneurysm model. J Neurosurg 2004:100:1041–1048.
11. Isoda H, Kinosada Y, Isogai S, Takehara Y, Ito T. Tagged MR imaging of intracranial aneurysm models. AJNR Am J Neuroradiol 1999:20:807–811.
12. Isoda H, Inagawa S, Takeda H, Isogai S, Takehara Y, Sakahara H. Preliminary study of tagged MR image velocimetry in a replica of an intracranial aneurysm. AJNR Am J Neuroradiol 2003:24:604–607.
13. Burleson AC, Strother CM, Turitto VT. Computer modeling of intracranial saccular and lateral aneurysms for the study of their hemodynamics. Neurosurgery 1995:37:774–782.
14. Steinman DA, Milner JS, Norley CJ, Lownie SP, Holdsworth DW. Image-based computational simulation of flow dynamics in a giant intracranial aneurysm. AJNR Am J Neuroradiol 2003:24:559–566.
15. Jou LD, Quick CM, Young WL, et al. Computational approach to quantifying hemodynamic forces in giant cerebral aneurysms. AJNR Am J Neuroradiol 2003:24:1804–1810.
16. Shojima M, Oshima M, Takagi K, et al. Magnitude and role of wall shear stress on cerebral aneurysm: computational fluid dynamic study of 20 middle cerebral artery aneurysms. Stroke 2004:35: 2500–2505.
17. Hassan T, Timofeev EV, Saito T, et al. Computational replicas: anatomic reconstructions of cerebral vessels as volume numerical grids at three-dimensional angiography. AJNR Am J Neuroradiol 2004:25:1356–1365.
18. DeWitt LD, Wechsler LR. Transcranial Doppler. Stroke 1988:19: 915–921.
19. Marks MP, Pelc NJ, Ross MR, Enzmann DR. Determination of cerebral blood flow with a phase-contrast cine MR imaging technique: evaluation of normal subjects and patients with arteriovenous malformations. Radiology 1992:182:467–476.
20. Markl M, Chan FP, Alley MT, et al. Time-resolved three-dimensional phase-contrast MRI. J Magn Reson Imaging 2003:17:499–506.
21. Markl M, Draney MT, Hope MD, et al. Time-resolved 3-dimensional velocity mapping in the thoracic aorta: visualization of 3-directional blood flow patterns in healthy volunteers and patients. J Comput Assist Tomogr 2004:28:459–468.
22. Bernstein MA, Zhou XJ, Polzin JA, et al. Concomitant gradient terms in phase contrast MR: analysis and correction. Magn Reson Med 1998:39:300–308.
23. Markl M, Bammer R, Alley MT, et al. Generalized reconstruction of phase contrast MRI: analysis and correction of the effect of gradient field distortions. Magn Reson Med. 2003:50:791–801.
24. Kerber CW, Liepsch D. Flow dynamics for radiologists. II. Practical considerations in the live human. AJNR Am J Neuroradiol 1994: 15:1076–1086.